Applied Energy 107 (2013) 191–208

Contents lists available at SciVerse ScienceDirect

Applied Energy

journal homepage: www.elsevier.com/locate/apenergy

Forecasting models for wind speed using wavelet, wavelet packet, time series and Artificial Neural Networks

Hui Liu [a,b,*], Hong-qi Tian [a], Di-fu Pan [a], Yan-fei Li [a,b]

[a] Key Laboratory for Traffic Safety on Track of Ministry of Education, School of Traffic and Transportation Engineering, Central South University, Changsha 410075, Hunan, China
[b] Institute of Automation, Faculty of Informatics and Electrical Engineering, University of Rostock, Rostock 18119, Mecklenburg-Vorpommern, Germany

HIGHLIGHTS

- Three new methods are proposed to predict wind speed for the wind power system.
- The Wavelet Packet-BFGS is better than the Wavelet Packet-ARIMA-BFGS.
- The Wavelet Packet-BFGS is better than the Wavelet-BFGS.
- They are compared to the Neuro-Fuzzy, ANFIS, RBF neural network and PM.

GRAPHICAL ABSTRACT

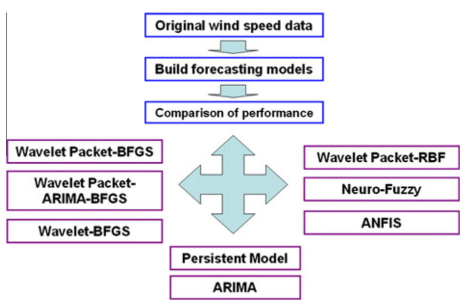

ARTICLE INFO

Article history:
Received 12 September 2012
Received in revised form 5 January 2013
Accepted 1 February 2013
Available online 16 March 2013

Keywords:
Wind speed predictions
Wind speed forecasting
Hybrid model
Signal decomposition
ANN
ARIMA

ABSTRACT

Wind speed forecasting is important for the security of wind power integration. Based on the theories of wavelet, wavelet packet, time series analysis and artificial neural networks, three hybrid models [Wavelet Packet-BFGS, Wavelet Packet-ARIMA-BFGS and Wavelet-BFGS] are proposed to predict the wind speed. The presented models are compared with some other classical wind speed forecasting methods including Neuro-Fuzzy, ANFIS (Adaptive Neuro-Fuzzy Inference Systems), Wavelet Packet-RBF (Radial Basis Function) and PM (Persistent Model). The results of three experimental cases show that: (1) the proposed three hybrid models have satisfactory performance in the wind speed predictions, and (2) the Wavelet Packet-ANN model is the best among them.

© 2013 Elsevier Ltd. All rights reserved.

Abbreviations: NWP, Numerical Weather Prediction; KF, Kalman Filter; PSO, Particle Swarm Optimization; ARIMA, Autoregressive Integrated Moving Average Model; VAR, Vector Autoregression Model; ANN, Artificial Neural Networks; GARCH, Generalized Autoregressive Conditional Heteroscedasticity; DRA, Different Regression Algorithm; RBF, Radial Basis Function; SVM, Support Vector Machines; RNN, Recurrent Neural Network; BT, Bayesian Theory; SBM, Structural Break Model; EMD, Empirical Mode Decomposition; FNN, Feed-forward Neural Network; BP, Back Propagation; TK, Taylor Kriging; SCMs, Soft Computing Models; BPNN, Backpropagation Neural Network; RBFNN, Radial Basis Function Neural Network; ANFIS, Adaptive Neuro-Fuzzy Inference Systems; HIFM, Hybrid Iterative Forecast Method; WD, Wavelet Decomposition; WPD, Wavelet Packet Decomposition; CWT, Continuous Wavelet Transform; DWT, Discrete Wavelet Transform; DWPT, Discrete Wavelet Packet Transform; AR, Autoregressive Model; MLP, Multilayer Perceptron; QPROP, Quick Propagation; RPROP, Resilient Propagation; BFGS, Broyden–Fletcher–Goldfarb–Shanno Quasi-Newton Back Propagation; PM, Persistent Model; EP, Evolutionary Programming; MAE, Mean Absolute Error; MAPE, Mean Absolute Percentage Error; MSE, Mean Square Error.

* Corresponding author at: Key Laboratory for Traffic Safety on Track of Ministry of Education, School of Traffic and Transportation Engineering, Central South University, Changsha 410075, Hunan, China.

E-mail address: csuliuhui@csu.edu.cn (H. Liu).

0306-2619/$ - see front matter © 2013 Elsevier Ltd. All rights reserved.
http://dx.doi.org/10.1016/j.apenergy.2013.02.002

1. Introduction

Wind energy has developed fast in the world. Just in China, the current total capacity of wind farms is 25805.3 MW [1]. To use the increasing wind energy effectively and safely, high-precision wind speed predictions are desired [2].

In the last 2 years, some new works have been made to realize wind speed predictions. Cassola and Burlando [3] proposed a method using NWP and KF to predict wind speed. In their works, the KF was used to filter the outputs of the NWP to get accurate results. Zhang et al. [4] employed four improved adaptive coefficient methods by PSO to forecast wind speed. Their simulated results showed the PSO promoted the forecasting performance. Erdem and Shi [5] made a comparison of one-step predictions by ARIMA, decomposed ARIMA, VAR and restricted VAR for two wind observation sites in North Dakota, USA. Liu et al. [6] compared an ARIMA-ANN model with an ARIMA-Kalman in wind speed multi-step predictions. They did not use the ARIMA to make the wind speed predictions directly but adopted it to choose the best parameters for the ANN and Kalman components. Liu et al. [7] presented a hybrid ARMA–GARCH method to forecast a series of 7-year hourly wind speed data in Colorado, USA. The results showed the performance of the ARMA-GARCH was satisfactory. Bouzgou and Benoudjit [8] proposed a multiple architecture system for wind speed predictions. In their system, three classical methods (DRA, RBF and SVM) were included. Cao et al. [9] discussed the forecasting accuracy of univariate and multivariate ARIMA models with their RNN counterparts. Jiang et al. [10] examined a new method for very short-term wind speed forecasting using BT and SBM. Guo et al. [11] combined EMD and FNN to build a hybrid EMD-FNN model for wind speed predictions. They concluded the performance of the hybrid model was better than that of the single FNN. Salcedo-Sanz et al. [12] studied wind speed predictions by SVM in a Spanish wind farm. To improve the performance of the classical SVM, two new hybrid methods (EP-SVM and PSO-SVM) were proposed. Their results showed that the two hybrid models both had satisfactory predictions. Guo et al. [13] proposed a method based on BP and method of idea of eliminating seasonal effects to forecast wind speed. The hybrid method forecasted the daily average wind speed more accurate than the BP model without adjustment. Liu et al. [14] investigated the performance of TK model in wind speed predictions. In their research, the results displayed the TK was better than the ARIMA. Shi et al. [15] compared the performance of the ARIMA, ANN and SVM models in wind speed short-term predictions. Their results showed both of the performance of the hybrid ARIMA-ANN and ARIMA-SVM were better than those of the single ARIMA, ANN and SVM models. Haque et al. [16] presented a performance analysis of short-term wind speed predictions using SCMs formulated on the BPNN, RBFNN and ANFIS. The research results showed their proposed hybrid methods were successful. The hybrid ANFIS model improved up to 48% forecasting accuracy compared with the single ANFIS. Amjady et al. [17] designed a new HIFM model for wind speed forecasting considering the interactions of temperature and wind speed. The forecasting results based on some real data from Iran and Spain confirmed that the HIFM was effective. Salim et al. [18] proposed five different adaptive Neuro-Fuzzy wind predictors and compared their performance in the East Coast of Egypt. More works about wind speed predictions can be found in Refs. [19–21].

Based on the upper literatures, it can be found that: (a) most of the latest methods are proposed by using more than one forecasting approaches to get better performance; (b) the modeling theories used in those works can be classified as three kinds: statistical methods, physical methods and intelligent methods. Every kind of methods has their own advantages and disadvantages. For example, the statistical methods are simpler than the physical and intelligent methods but with lower accuracy; (c) when a new method is proposed, it should be seriously compared with some existing models to prove its contributions; and (d) besides the forecasting accuracy, the multi-step ahead capacity of models is also emphasized in wind speed predictions. Some similar conclusions can also be made by reviewing the literatures of wind power/load [22–28] and electricity price [29–31] predictions.

From the literatures [1–21], it can also be seen that in the wind speed predictions there are at least two kinds of effective ideas to possibly get high-precision results. One is to use the other methods to improve the forecasting capacities of the principal methods. After the necessary optimization, the principal methods could handle with the non-stationary wind speed data better. For instance, the PSO has been adopted to choose the best initial parameters of the SVM in the wind speed predictions [12]. In this kind, the other methods directly promote the forecasting performance of the principal methods. The other one is to utilize the other methods to decrease the forecasting difficulty of the original wind speed. For example, the EMD has been selected to decrease the non-stationary degree of the original wind speed in the wind speed predictions [11]. In this kind, the other methods do not directly promote the forecasting performance of the principal methods. In

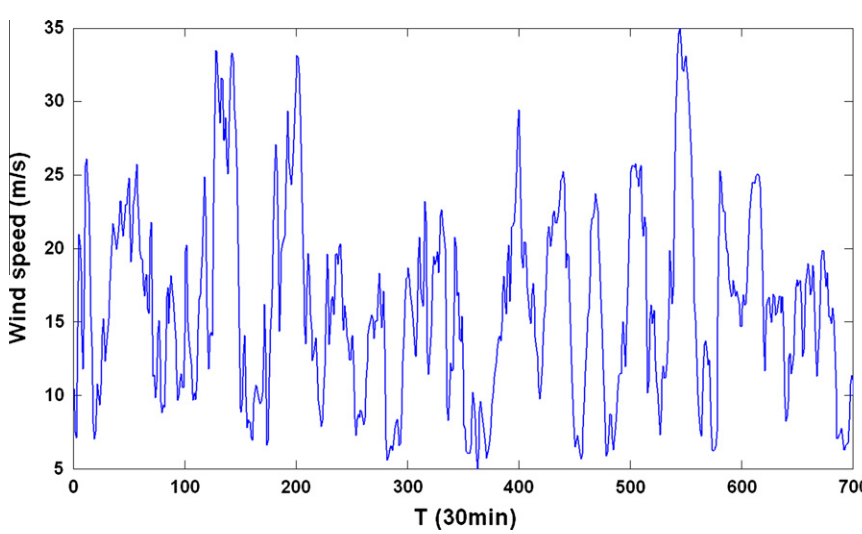

Fig. 1. A section of original wind speed data.

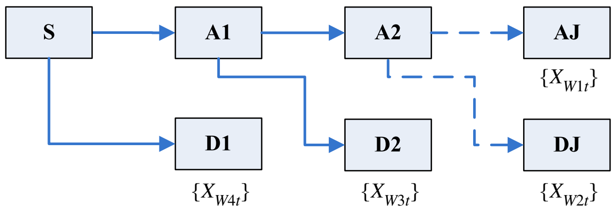

Fig. 2. Computational process of DWT.

this study we would like to study the second classification. In signal decomposing fields, the WD [32] and the WPD [33] are generally recognized. In this paper, they are selected to build hybrid models with the representative one in intelligent methods-ANN and the classical one in statistical methods-ARIMA to predict three sections of wind speed data. Additional a comparison of the proposed hybrid methods and other important forecasting methods (including ANFIS, Neuro-Fuzzy, RBF and PM) will be provided.

This paper is organized as follows: Section 2 states the framework of this study; Section 3 demonstrates the computational steps of the proposed hybrid methods using a real section of wind speed data; Section 4 compares the proposed hybrid methods with other methods; and Section 5 provides additional two forecasting cases; and Section 6 concludes the results of this study.

2. Framework of modeling

The framework of this study is demonstrated as follows:

(1) Use the wavelet packet and wavelet to decompose an original wind speed series into a number of sub-series, respectively.

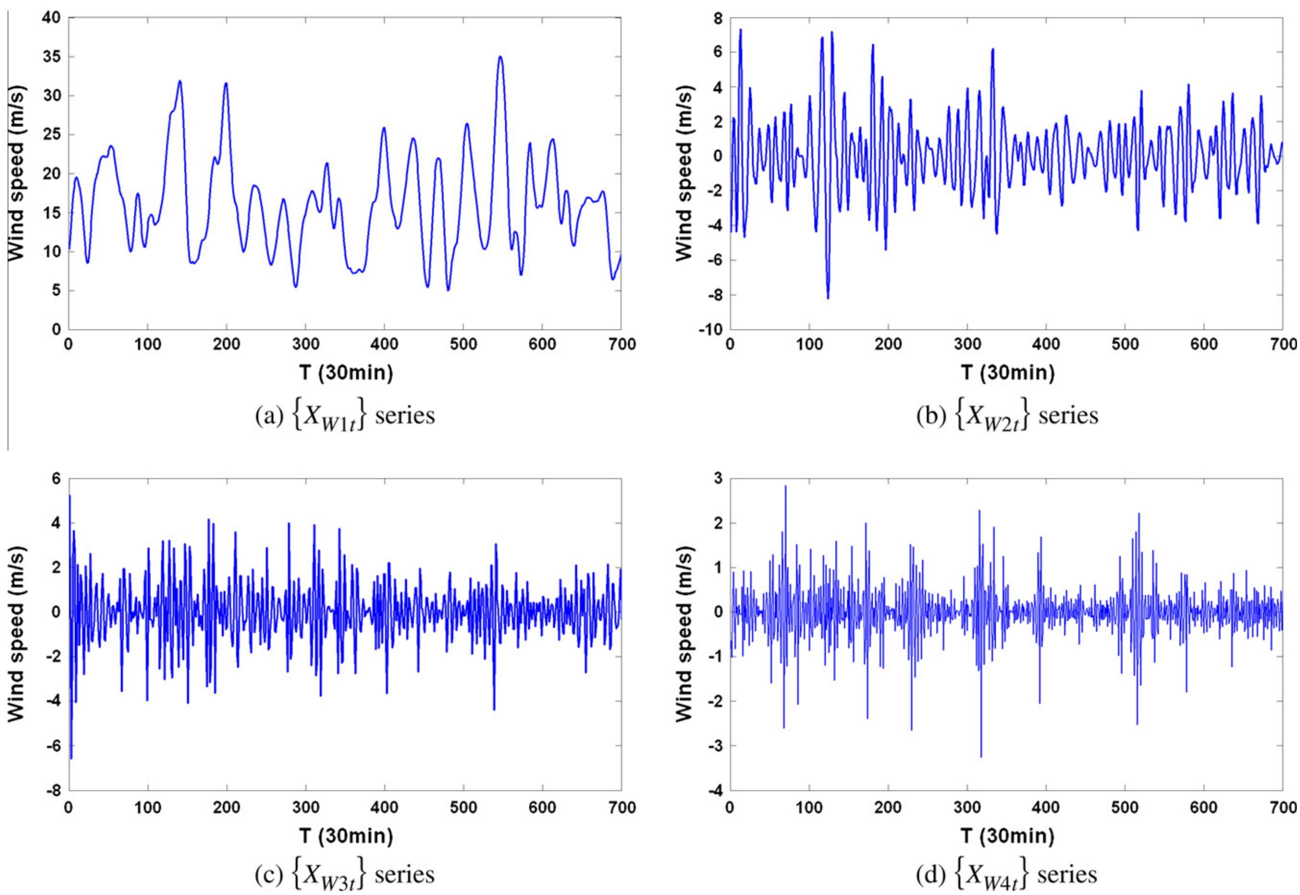

Fig. 3. DWT results.

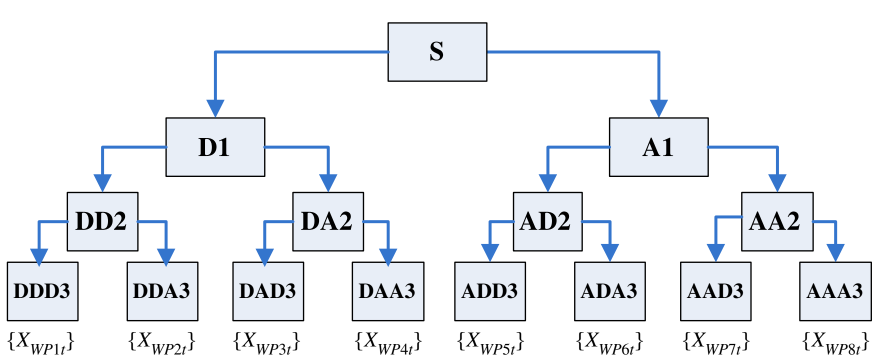

Fig. 4. Process of DWPT.

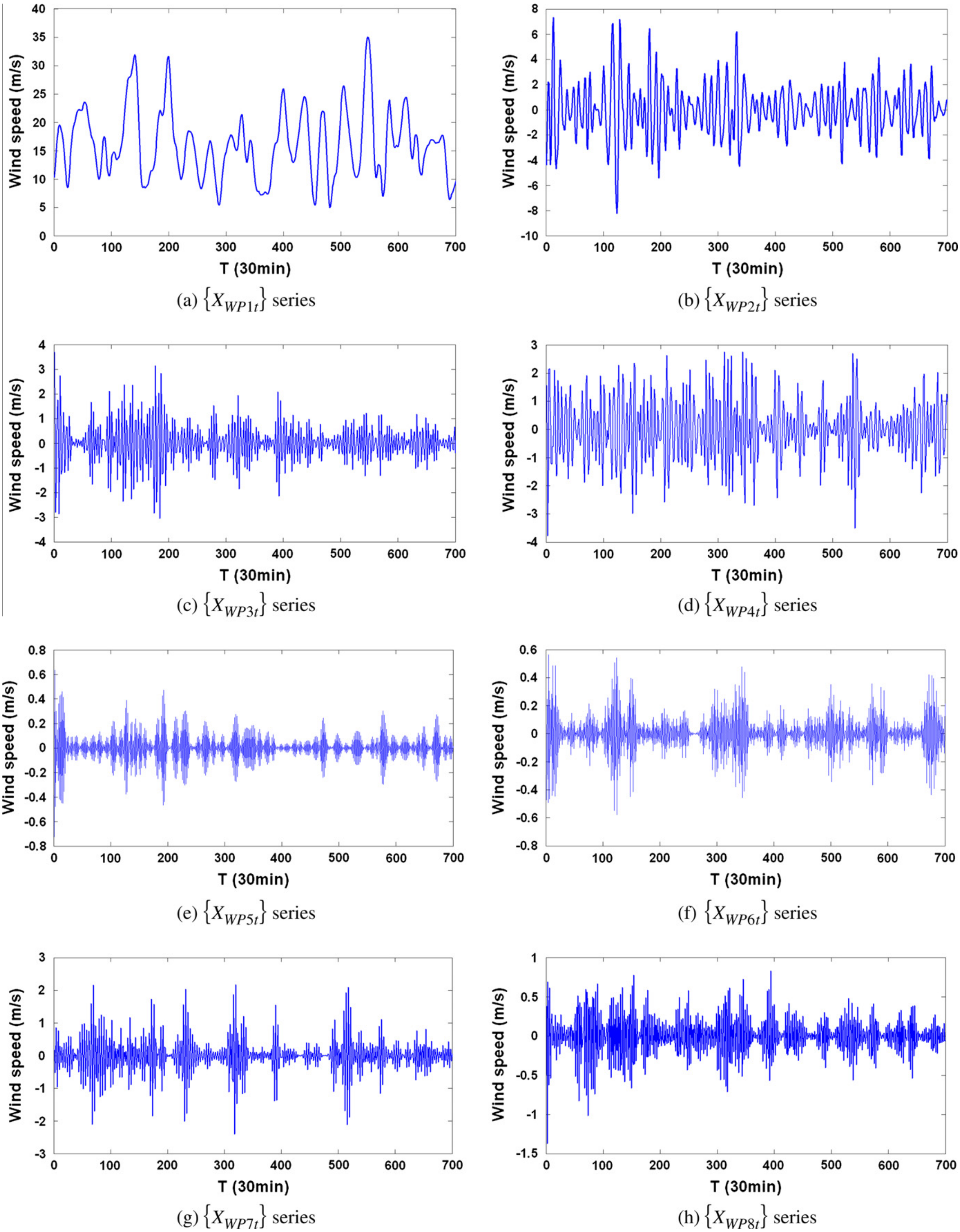

(a) $\{X_{WP1t}\}$ series

(b) $\{X_{WP2t}\}$ series

(c) $\{X_{WP3t}\}$ series

(d) $\{X_{WP4t}\}$ series

(e) $\{X_{WP5t}\}$ series

(f) $\{X_{WP6t}\}$ series

(g) $\{X_{WP7t}\}$ series

(h) $\{X_{WP8t}\}$ series

Fig. 5. DWPT results.

Table 1
Results of the training algorithm experiment.

Kind of training algorithm	Estimation indexes	
	MAE (m/s)	RMSE (m/s)
BP	0.0460	0.9728
QPROP	0.0454	0.8470
RPROP	0.0222	0.4084
BFGS	0.0082	0.1482

(2) Apply the time series method to build ARIMA forecasting models for every sub-series. Employ those ARIMA models to determine the numbers of inputting and outputting neurons for the ANN models in each sub-series.
(3) Do a group of trial experiments to select the best training algorithm and numbers of hidden neurons for those ANN models.
(4) Utilize the built ANN models to do the multi-step forecasting in each sub-series.
(5) Conduct aggregate calculation for the multi-step forecasting results in sub-series to obtain the final forecast for the original wind speed series.
(6) Hybrid forecasting models are built based on different combinations of the upper four modeling methods.
(7) To check their performance, the proposed hybrid models will be compared with other existing forecasting models, including Neuro-Fuzzy model, ANFIS model, Wavelet Packet-RBF model and PM model.
(8) To make a completed comparison, three groups of actual half-hourly wind speed series from Chinese Qinghai Wind Farm at different seasons are provided.

3. Modeling steps of the proposed hybrid models

3.1. Wind speed measurement

Fig. 1 shows an actual half-hourly wind speed series (including 700 data) sampled from Chinese Qinghai Wind Farm. Those data are collected from December 20, 2011 to January 5, 2012. In this section of wind speed data, the 1st–600th samplings will be used

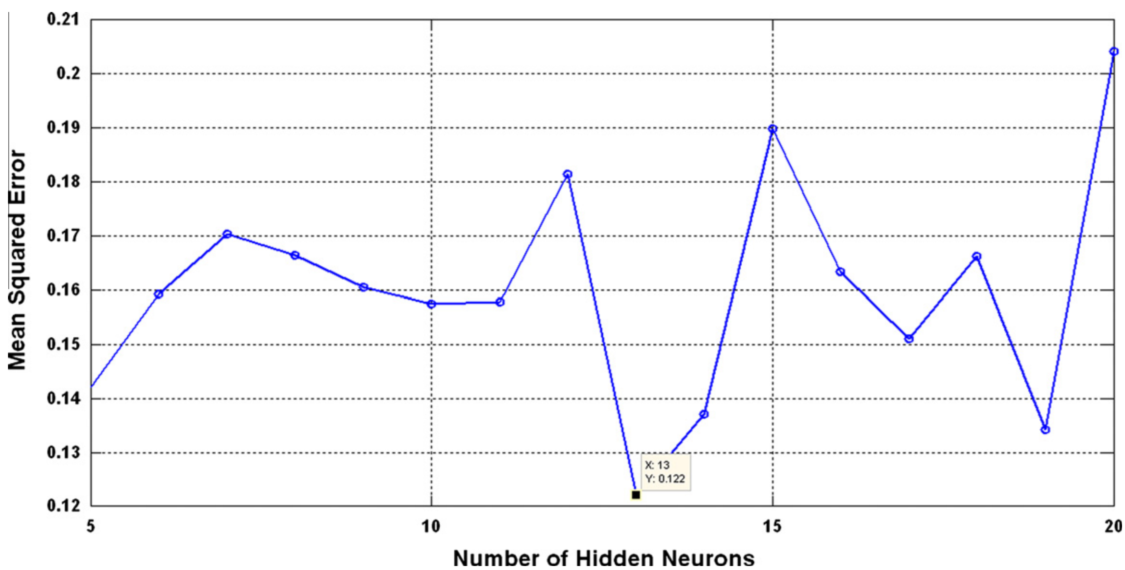

Fig. 6. The MSE errors with different numbers of hidden neurons.

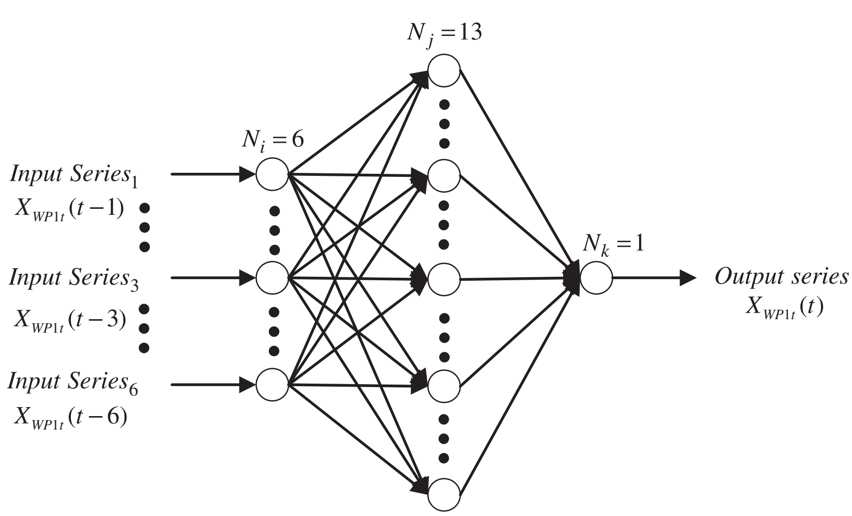

Fig. 7. Completed three-layer ANN.

to build forecasting models and the following 601st–700th samplings will be loaded into the built models to verify their forecasting performance.

3.2. Wind speed decomposition

3.2.1. Wavelet Decomposition

WD is a mathematical technology used to analyze signals by decomposition into various frequencies [32]. In this study, the WD is employed to process an original wind speed series into a group of sub-series.

A CWT for an original signal $f(t)$ with respect to a mother wavelet function $\psi(t)$ can be defined as [32]:

$$\mathrm{CWT}_f(a,b) = \langle f(t), \psi_{a,b}(t)\rangle = \int_{-\infty}^{+\infty} f(t)\frac{1}{\sqrt{|a|}}\psi^*\left(\frac{t-b}{a}\right)dt \tag{1}$$

where $*$ denotes the complex conjugate, a is a scale coefficient and b is a translation coefficient.

The CWT has a digital counterpart, the DWT: to provide necessary information whilst reducing calculation cost, the following sample is used:

$$\begin{cases} a = 2^j \\ b = k2^j \end{cases} \tag{2}$$

where j, k are the scale coefficient and the translation coefficient, respectively. In this study Mallat algorithm is executed for the multi-solution DWT computation, which implements the DWT process using a series of filters. Suppose S is an original wind speed series, the computational process of a DWT can be demonstrated as shown in Fig. 2, where J is the decomposed level. To facilitate the latter calculation, the first detail sub-series is recorded as $\{X_{W4t}\}$ series, the second detail sub-series recorded as $\{X_{W3t}\}$ series, the third detail sub-series recorded as $\{X_{W2t}\}$ series and the third approximation sub-series recorded as $\{X_{W1t}\}$ series. Fig. 3 displays the DWT results of the original wind speed series given in Fig. 1.

3.2.2. Wavelet Packet Decomposition

DWPT is a special wavelet transform where the original signal will pass through more filters than the DWT. In a DWT process, only the previous approximation coefficients will be decomposed by a group of low and high quadrature mirror filters [33]. In the DWPT, both of the previous approximation and detail coefficients will be decomposed. The decomposition process of a DWPT can be described as shown in Fig. 4. Fig. 5 displays the DWPT results of the same original wind speed series in Fig. 1.

3.3. ANN modeling

In ANN theory, there are kinds of algorithms to train the MLP architecture, including BP, QPROP [34], RPROP [35] and BFGS [36]. To select the best training algorithm, an experiment is made by using the 1st–600th samplings of the original wind speed in Fig. 1, with the results displayed in Table 1. From Table 1, it can be found that the BFGS algorithm is the best for the ensuing ANN modeling.

In this study a neural network with three layers is adopted to guarantee that the built models can output the forecasting results fast. Besides the model structure, the number of neurons in every layer is important. A time series method is used to choose the best numbers of neurons for a three-layer ANN model. The best time series model for the 1st–600th data of the $\{X_{WP1t}\}$ series is chosen as ARIMA (5,1,0), with the corresponding equation as:

$$\begin{aligned} X_{WP1t}(t) = {} & 3.0157X_{WP1t}(t-1) - 3.6297X_{WP1t}(t-2) \\ & + 2.6589X_{WP1t}(t-3) - 1.7931X_{WP1t}(t-4) \\ & + 0.9908X_{WP1t}(t-5) - 0.2427X_{WP1t}(t-6) \\ & + a_{WP1t}, \\ t = {} & 7,8,9,\ldots,600. \end{aligned} \tag{3}$$

Eq. (3) states the data correlation in the $\{X_{WP1t}\}$ series with a white noise series $\{a_{WP1t}\}$. Using Eq. (3), the following numbers of neurons can be decided for the 1st–600th data of the $\{X_{WP1t}\}$

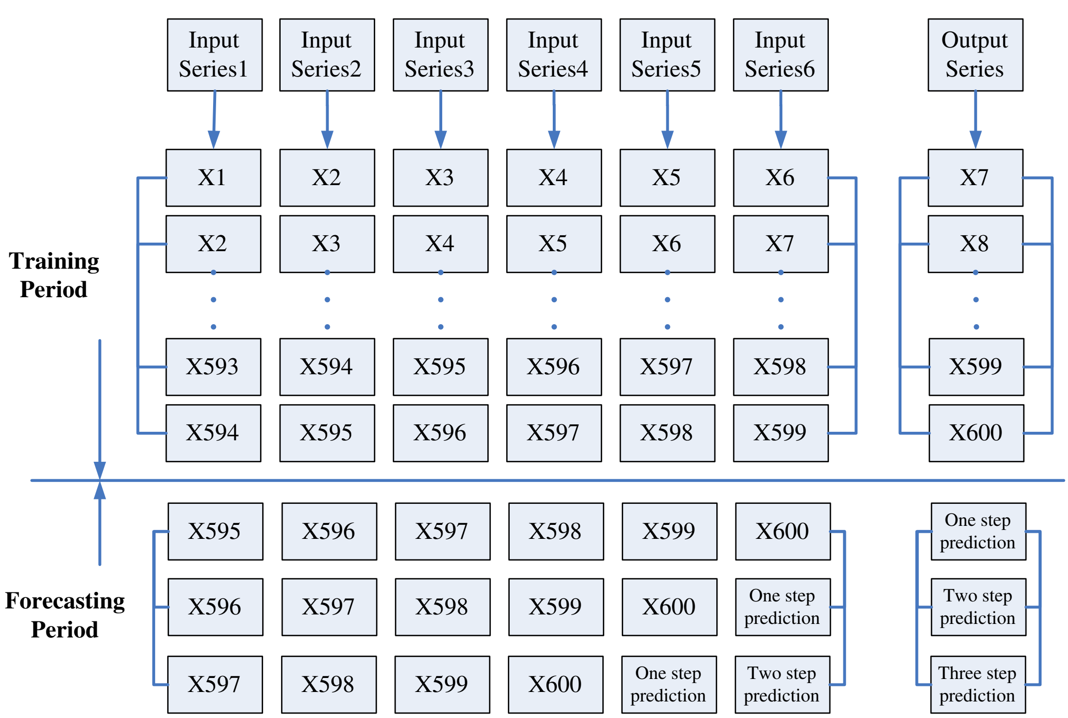

Fig. 8. Data format of inputting and outputting.

Table 2
Identified results of the time series models for the other sub-series.

Sub-series	Time series models
$\{X_{WP2t}\}$ series	$X_{WP2t}(t) = 3.1556X_{WP2t}(t-1) - 4.1822X_{WP2t}(t-2) + 3.6554X_{WP2t}(t-3) - 3.1624X_{WP2t}(t-4) + 2.7855X_{WP2t}(t-5) - 1.9963X_{WP2t}(t-6) + 0.9518X_{WP2t}(t-7) - 0.2074X_{WP2t}(t-8) + a_{WP2t}, \quad t = 9, 10, 11, \ldots, 600$
$\{X_{WP3t}\}$ series	$X_{WP3t}(t) = 3.0607X_{WP3t}(t-1) - 3.5153X_{WP3t}(t-2) + 2.0658X_{WP3t}(t-3) - 1.2014X_{WP3t}(t-4) + 1.1297X_{WP3t}(t-5) - 0.5298X_{WP3t}(t-6) - 0.5695X_{WP3t}(t-7) + 0.5429X_{WP3t}(t-8) + 0.8179X_{WP3t}(t-9) - 1.2601X_{WP3t}(t-10) + 0.4591X_{WP3t}(t-11) + a_{WP3t}, \quad t = 12, 13, 14, \ldots, 600$
$\{X_{WP4t}\}$ series	$X_{WP4t}(t) = 2.0775X_{WP4t}(t-1) - 3.2847X_{WP4t}(t-2) + 3.9475X_{WP4t}(t-3) - 4.8109X_{WP4t}(t-4) + 5.1907X_{WP4t}(t-5) - 4.6120X_{WP4t}(t-6) + 3.6376X_{WP4t}(t-7) - 2.5141X_{WP4t}(t-8) + 1.8272X_{WP4t}(t-9) - 0.7845X_{WP4t}(t-10) + 0.2048X_{WP4t}(t-11) + 0.1209X_{WP4t}(t-12) + a_{WP4t}, \quad t = 13, 14, 15, \ldots, 600$
$\{X_{WP5t}\}$ series	$X_{WP5t}(t) = -0.2678X_{WP5t}(t-1) + 1.1049X_{WP5t}(t-2) + 0.2479X_{WP5t}(t-3) - 0.1406X_{WP5t}(t-4) + 0.1121X_{WP5t}(t-5) - 0.0963X_{WP5t}(t-6) + 0.0650X_{WP5t}(t-7) - 0.0271X_{WP5t}(t-8) - 0.0389X_{WP5t}(t-9) + 0.0765X_{WP5t}(t-10) - 0.0352X_{WP5t}(t-11) - 0.0073X_{WP5t}(t-12) + 0.0327X_{WP5t}(t-13) - 0.0259X_{WP5t}(t-14) + a_{WP5t}, \quad t = 15, 16, 17, \ldots, 600$
$\{X_{WP6t}\}$ series	$X_{WP6t}(t) = 1.9625X_{WP6t}(t-1) - 3.2987X_{WP6t}(t-2) + 4.4084X_{WP6t}(t-3) - 4.5099X_{WP6t}(t-4) + 4.4832X_{WP6t}(t-5) - 3.5863X_{WP6t}(t-6) + 2.7742X_{WP6t}(t-7) - 2.2053X_{WP6t}(t-8) + 1.7184X_{WP6t}(t-9) - 1.3879X_{WP6t}(t-10) + 1.0861X_{WP6t}(t-11) - 0.6732X_{WP6t}(t-12) + 0.3673X_{WP6t}(t-13) - 0.1389X_{WP6t}(t-14) + a_{WP6t}, \quad t = 15, 16, 17, \ldots, 600$
$\{X_{WP7t}\}$ series	$X_{WP7t}(t) = 1.9689X_{WP7t}(t-1) - 3.3229X_{WP7t}(t-2) + 4.4591X_{WP7t}(t-3) - 4.5950X_{WP7t}(t-4) + 4.6036X_{WP7t}(t-5) - 3.7359X_{WP7t}(t-6) + 2.9581X_{WP7t}(t-7) - 2.4359X_{WP7t}(t-8) + 2.0089X_{WP7t}(t-9) - 1.7564X_{WP7t}(t-10) + 1.5104X_{WP7t}(t-11) - 1.0953X_{WP7t}(t-12) + 0.7469X_{WP7t}(t-13) - 0.4065X_{WP7t}(t-14) + 0.1537X_{WP7t}(t-15) - 0.0619X_{WP7t}(t-16) + a_{WP7t}, \quad t = 17, 18, 19, \ldots, 600$
$\{X_{WP8t}\}$ series	$X_{WP8t}(t) = -0.4591X_{WP8t}(t-1) - 0.3323X_{WP8t}(t-2) + 0.6988X_{WP8t}(t-3) - 0.1318X_{WP8t}(t-4) + 0.4048X_{WP8t}(t-5) + 0.4578X_{WP8t}(t-6) + 0.7263X_{WP8t}(t-7) - 0.1313X_{WP8t}(t-8) - 0.3094X_{WP8t}(t-9) - 0.0438X_{WP8t}(t-10) + 0.0954X_{WP8t}(t-11) - 0.0601X_{WP8t}(t-12) - 0.1829X_{WP8t}(t-13) + 0.0583X_{WP8t}(t-14) + 0.1286X_{WP8t}(t-15) + 0.0807X_{WP8t}(t-16) + a_{WP8t}, \quad t = 17, 18, 19, \ldots, 600$

Table 3
Input numbers of the ANN models for the other sub-series.

Sub-series	Input numbers of ANN models
$\{X_{WP2t}\}$ series	8
$\{X_{WP3t}\}$ series	11
$\{X_{WP4t}\}$ series	12
$\{X_{WP5t}\}$ series	14
$\{X_{WP6t}\}$ series	14
$\{X_{WP7t}\}$ series	16
$\{X_{WP8t}\}$ series	16

series: Number of input neurons $N_i = 6$; number of output neurons $N_k = 1$. As computational results given in Fig. 6, an experiment is provided to choose the best number of hidden neurons by using the 1st–600th samplings of the $\{X_{WP1t}\}$ series. As shown in Fig. 6, the best number of hidden neurons in this experiment is 13.

After finishing the upper steps, a three-layer ANN model has been completed as shown in Fig. 7. The corresponding data format can be defined in Fig. 8.

The time series models for the other sub-series in Fig. 5 can be identified by referring to the computational steps of the $\{X_{WP1t}\}$ series. The identified results are given in Table 2.

Based on the identified results given in Table 2, the input numbers of the other ANN models can be decided as shown in Table 3.

3.4. Aggregate calculation of sub-series

Equation of aggregate calculation for sub series is given as:

$$\begin{aligned} \hat{v}_t(t) = {} & \rho_1\widehat{X}_{PW1t}(t) + \rho_2\widehat{X}_{PW2t}(t) + \rho_3\widehat{X}_{PW3t}(t) + \rho_4\widehat{X}_{PW4t}(t) \\ & + \rho_5\widehat{X}_{PW5t}(t) + \rho_6\widehat{X}_{PW6t}(t) + \rho_7\widehat{X}_{PW7t}(t) + \rho_8\widehat{X}_{PW8t}(t), \\ t = {} & 601, 602, \ldots, 700 \end{aligned} \tag{4}$$

where the aggregate coefficient $\rho_1 = \rho_2 = \cdots = \rho_7 = \rho_8 = 1$, and t is the sampling time.

4. Forecast results and comparative analysis

4.1. Wavelet Packet-BFGS vs. Wavelet-BFGS vs. BFGS

The first group of hybrid models by using wavelet packet, wavelet and ANN is provided to make wind speed multi-step predictions, including the hybrid Wavelet Packet-BFGS model, the hybrid Wavelet-BFGS model and the pure BFGS model. The hybrid Wavelet Packet-BFGS model makes the predictions by establishing multi ANN models using BFGS training algorithm in every DWPT sub-series. The hybrid Wavelet-BFGS model does the predictions by building multi ANN models using BFGS training algorithm in every DWT sub-series.

To make a fair comparison of the different hybrid models, the key parameters of the ANN component are kept the same in every combination. The parameters are listed as follows:

(a) Number of input neurons N_i: 6.
(b) Number of hidden layer neurons N_j: 13.
(c) Number of output neurons N_k: 1.
(d) Number of iterative steps: 594.
(e) Value of the learning rate: 0.05.

Figs. 9–11 show the results at 601st–700th data of one-step, two-step and three-step predictions. The estimated results of their

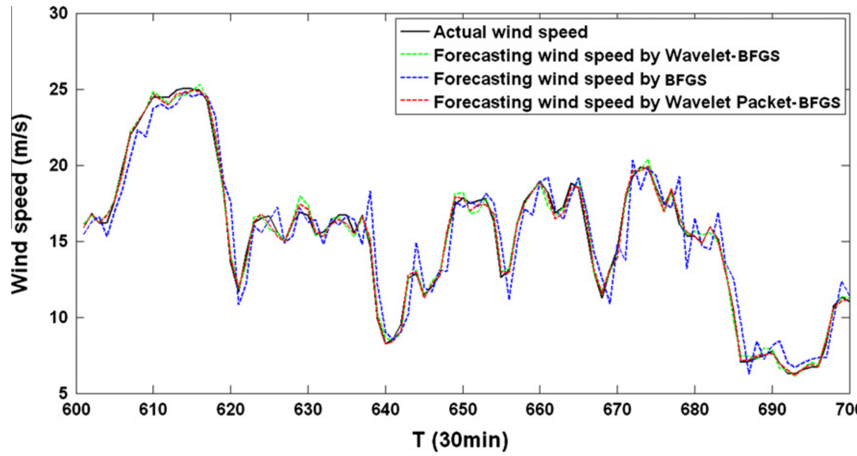

Fig. 9. Results of one-step prediction (1).

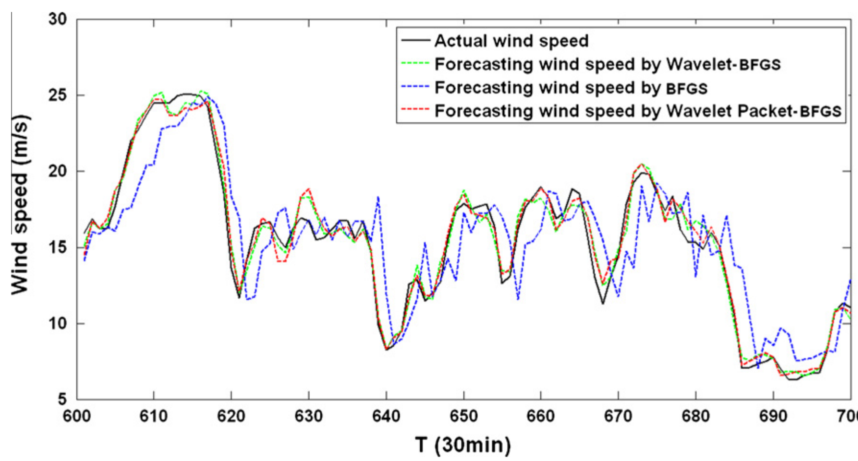

Fig. 10. Results of two-step prediction (1).

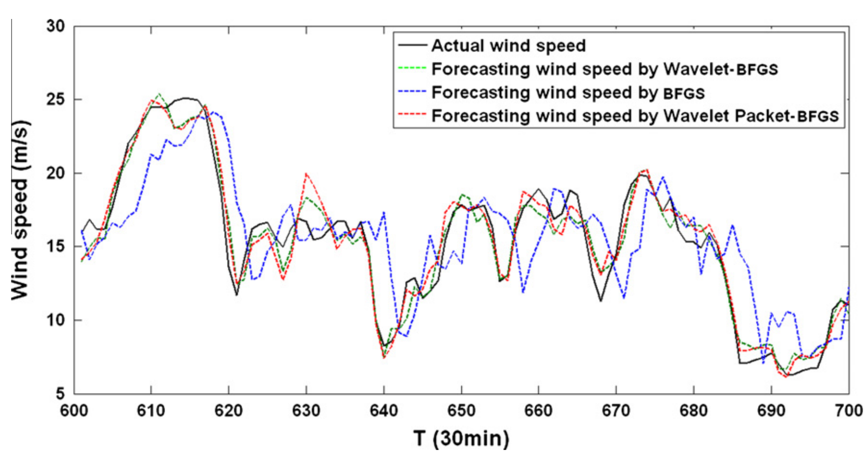

Fig. 11. Results of three-step prediction (1).

Table 4
Analysis of the forecasting results shown in Figs. 9–11.

Indexes	Wavelet Packet-BFGS			Wavelet-BFGS model			BFGS model		
	1-step	2-step	3-step	1-step	2-step	3-step	1-step	2-step	3-step
MAE (m/s)	0.2174	0.5629	0.9040	0.3091	0.6322	0.8937	1.0137	2.0087	2.5170
MAPE (%)	1.48	3.83	6.38	2.18	4.32	6.44	7.45	15.08	19.60
MSE (m/s)	0.2777	0.7203	1.1131	0.3936	0.7766	1.1358	1.3285	2.5735	3.2146

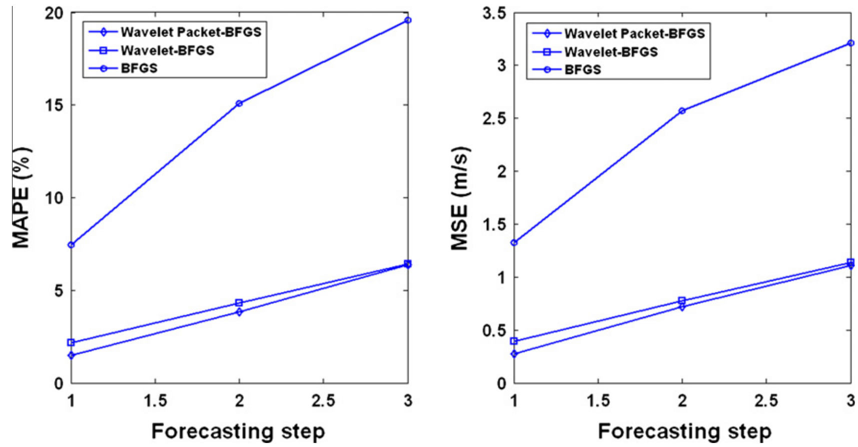

Fig. 12. Changing Law of the MAPE and MSE errors in Table 4.

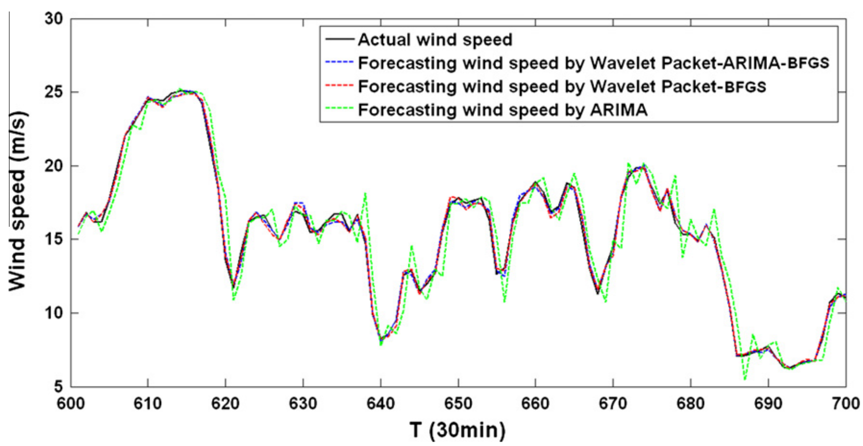

Fig. 13. Results of one-step prediction (2).

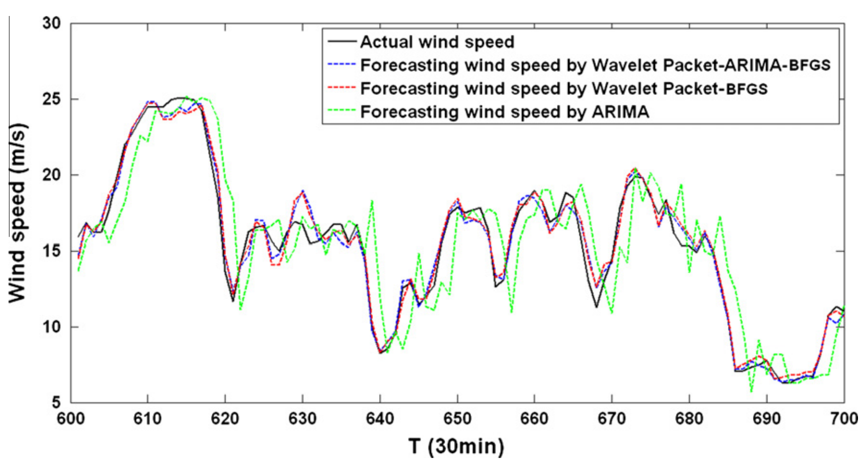

Fig. 14. Results of two-step prediction (2).

predictions are given in Table 4. The MAPE and MSE errors in Table 4 are drawn in Fig. 12.

From Figs. 9–11 and Table 4, it can be seen that: (a) this hybrid forecasting idea adopted in this study is effective to predict the non-stationary wind speed, both of the Wavelet Packet-BFGS and the Wavelet-BFGS get satisfactory performance. Taking the three-step forecasting results for example, the MAPE errors of the traditional BFGS neural network, the Wavelet Packet-BFGS and the Wavelet-BFGS are 19.60%, 6.38% and 6.44%, respectively. The reason of this results is because the wavelet and wavelet packet

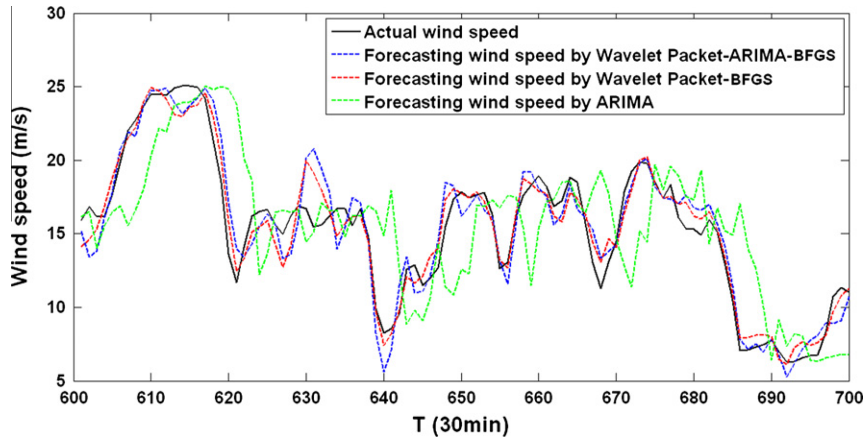

Fig. 15. Results of three-step prediction (2).

Table 5
Analysis of the forecasting results shown in Figs. 13–15.

Indexes	Wavelet Packet-ARIMA-BFGS			Wavelet Packet-BFGS			ARIMA model		
	1-step	2-step	3-step	1-step	2-step	3-step	1-step	2-step	3-step
MAE (m/s)	0.2352	0.5817	1.1866	0.2174	0.5629	0.9040	0.9742	1.9235	3.0400
MAPE (%)	1.59	3.97	8.48	1.48	3.83	6.38	7.17	14.42	23.49
MSE (m/s)	0.2956	0.7473	1.5465	0.2777	0.7203	1.1358	1.3224	2.5601	3.9920

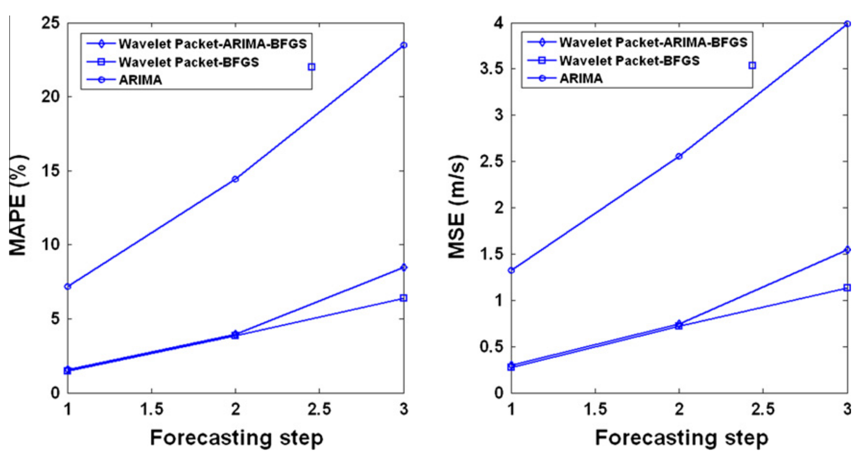

Fig. 16. Changing Law of the MAPE and MSE errors in Table 5.

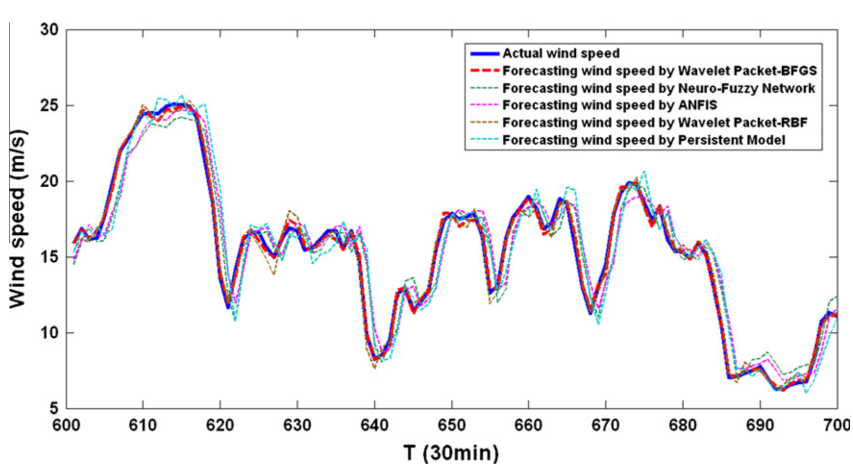

Fig. 17. Results of one-step prediction (3).

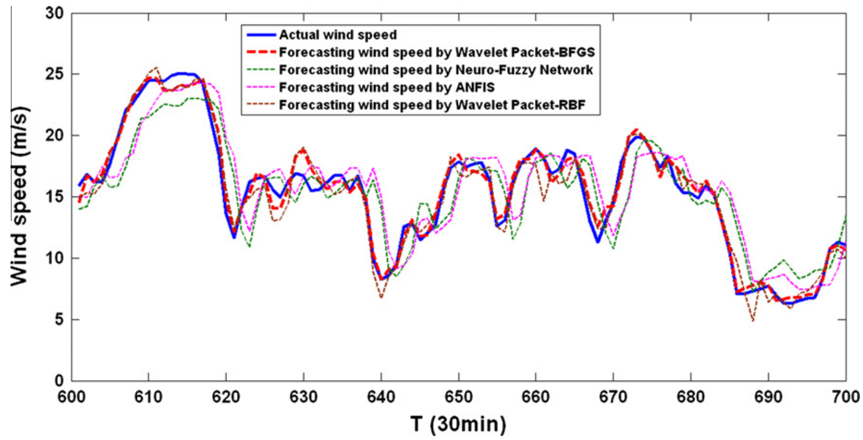

Fig. 18. Results of two-step prediction (3).

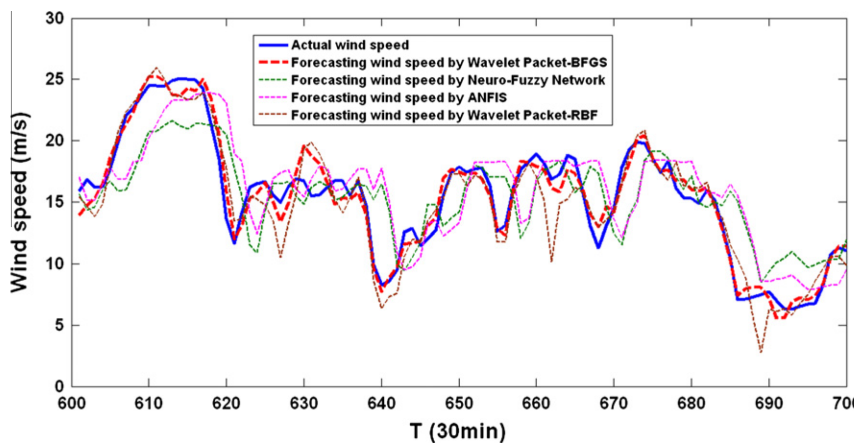

Fig. 19. Results of three-step prediction (3).

Table 6
Analysis of the forecasting results shown in Figs. 17–19.

Indexes	Wavelet Packet-BFGS			Neuro-Fuzzy network			ANFIS		
	1-step	2-step	3-step	1-step	2-step	3-step	1-step	2-step	3-step
MAE (m/s)	0.2174	0.5629	0.9040	1.1693	2.0985	2.6149	1.1816	2.0218	2.6672
MAPE (%)	1.48	3.83	6.38	8.75	16.01	20.71	8.80	15.56	20.87
MSE (m/s)	0.2777	0.7203	1.1358	1.4789	2.5942	3.2987	1.5773	2.6775	3.4255

Indexes	Wavelet Packet-RBF			Persistent Model		
	1-step	2-step	3-step	1-step	2-step	3-step
MAE (m/s)	0.3617	0.8684	1.3571	1.2442	–	–
MAPE (%)	2.63	6.34	10.18	8.97	–	–
MSE (m/s)	0.4588	1.0960	1.7820	1.7050	–	–

decompose the non-stationary wind speed into a series of relatively stable sub-layers which lower the forecasting difficulty of the ANN in the ensuing forecasting computation; and (b) in this case, the Wavelet Packet-BFGS has better performance than the Wavelet-BFGS. The phenomenon can be explained as: the wavelet packet decomposes the original wind speed signal better than the Wavelet. The former one handles both of the appropriate and detailed components in every layer but the latter one only copes with the appropriate components.

From Fig. 12, it can be found that the performance difference between the Wavelet Packet-BFGS and the Wavelet-BFGS is not significant.

4.2. Wavelet Packet-ARIMA-BFGS vs. Wavelet Packet-BFGS vs. ARIMA

The second group of hybrid models by using wavelet packet, ANN and ARIMA is established to make wind speed multi-step predictions, including the hybrid Wavelet Packet-ARIMA-BFGS model, the hybrid Wavelet Packet-BFGS model and the pure ARIMA model. The calculation steps of the hybrid Wavelet Packet-ARIMA-BFGS model are given as follows: Build the ARIMA models in the approximation sub-series and the ANN model with BFGS training algorithm in the detail sub-series, respectively; make the multi-step predictions in every sub-series using the built models; conduct

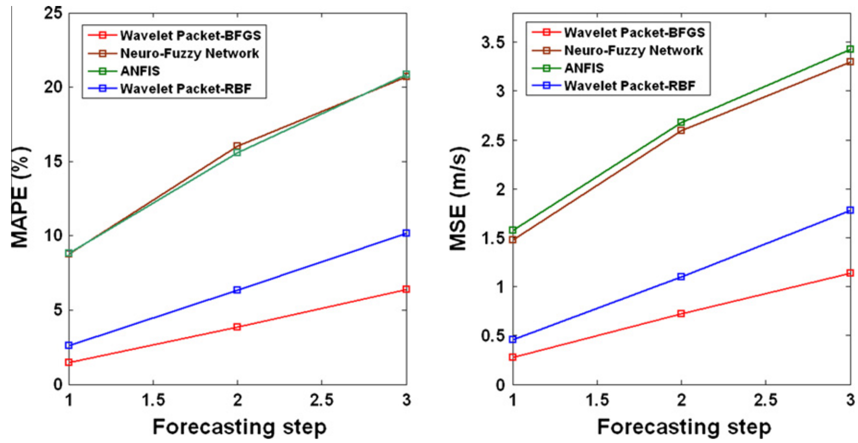

Fig. 20. Changing Law of the MAPE and MSE errors in Table 6.

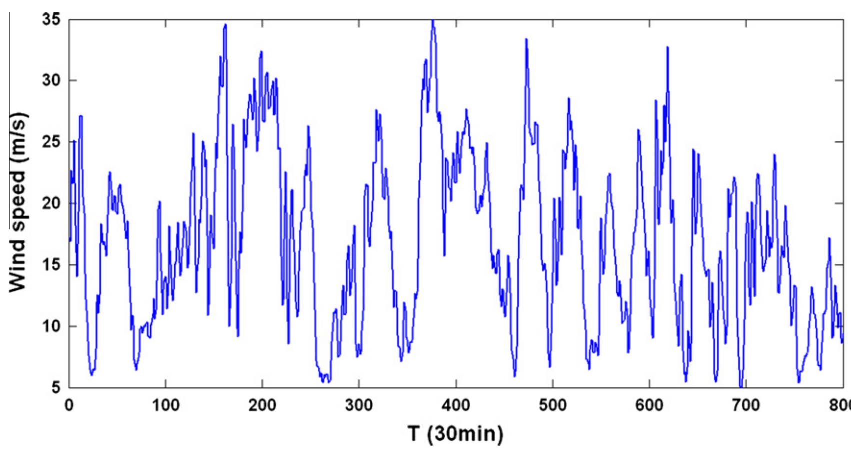

Fig. 21. Original wind speed series (2).

aggregate calculation of the sub-series forecasting values to get the final wind speed predictions.

Figs. 13–15 show the results at 601st–700th data of one-step, two-step and three-step predictions. The estimated results of the predictions are given in Table 5. The MAPE and MSE errors in Table 5 are displayed in Fig. 16.

From Figs. 13–15 and Table 5, it can be seen that: (a) Similar to the results given in Section 4.1, the bigger the number of forecast steps, the lower the accuracy. This is an objective law in any wind speed forecasting method; (b) the performance of the Wavelet Packet-BFGS and the Wavelet Packet-ARIMA-BFGS is much better than that of the pure ARIMA network in every step predictions; and (c) the performance of the Wavelet Packet-BFGS is close to that of the Wavelet Packet-ARIMA-BFGS in one-step and two-step predictions. The reason of this phenomenon can be given as: the former one builds all the BFGS neural network in all sub-series but

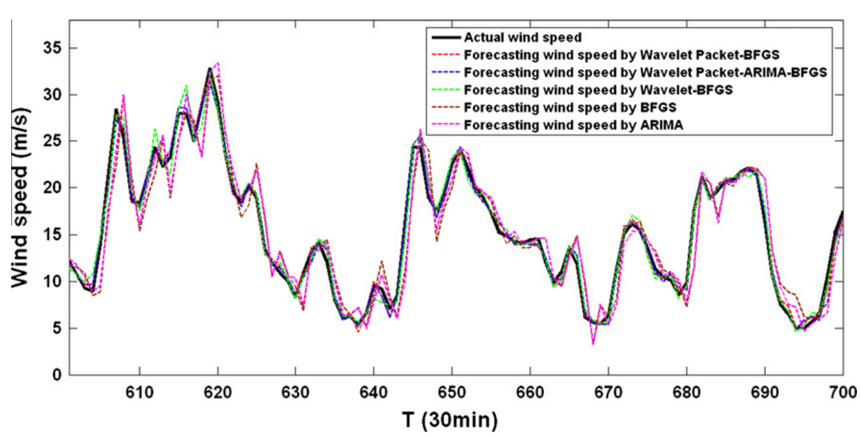

Fig. 22. Results of one-step prediction (4).

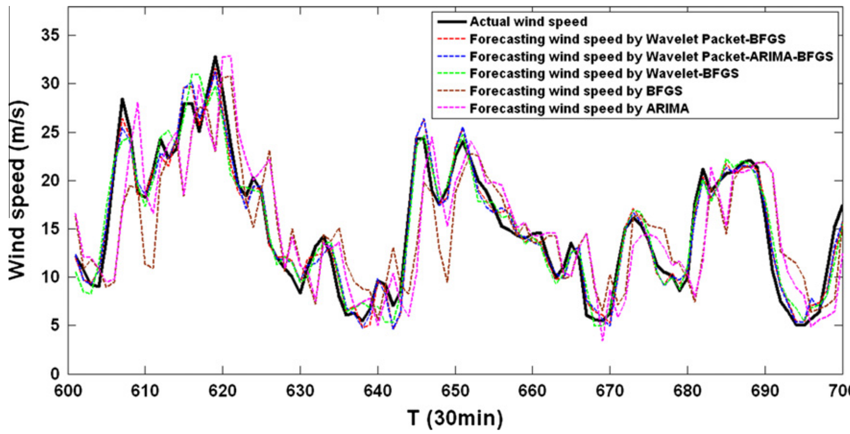

Fig. 23. Results of two-step prediction (4).

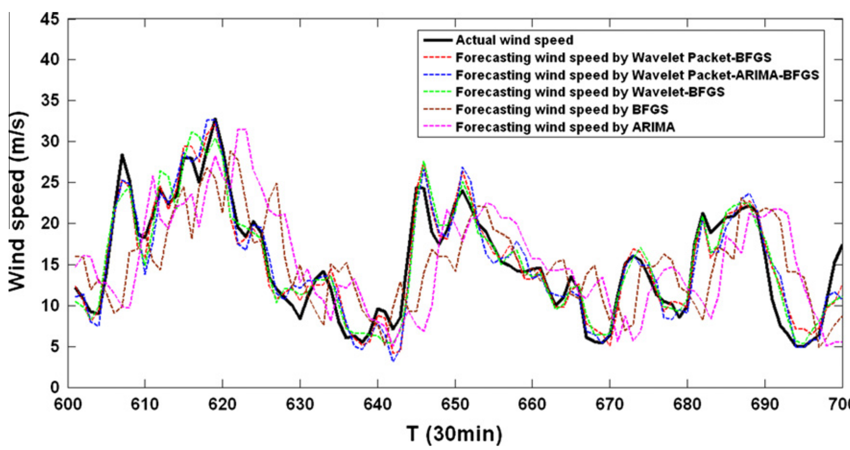

Fig. 24. Results of three-step prediction (4).

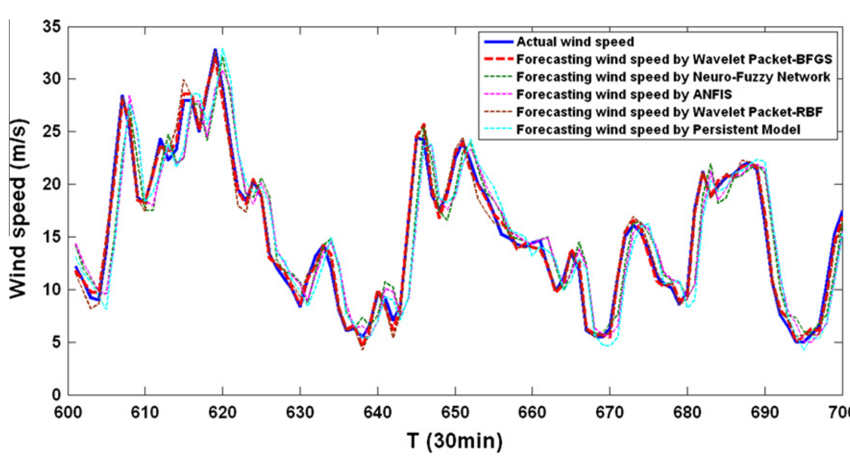

Fig. 25. Results of one-step prediction (5).

the latter one builds the BFGS neural network in detailed sub-series and establishes the ARIMA models in appropriate sub-series. In the appropriate sub-series which are more stable, the performance of the BFGS is originally close to the performance of the ARIMA. However from Fig. 16, it can be found that in the three-step predictions, the Wavelet Packet-BFGS is obviously better than the Wavelet Packet-ARIMA-BFGS. This is because the robust performance of the BFGS network is better than that of the ARIMA.

4.3. Wavelet Packet-BFGS Neural Network vs. Neuro-Fuzzy vs. ANFIS vs. Wavelet Packet-RBF vs. Persistent Model

To estimate the performance of the proposed models, the best one (Wavelet Packet-BFGS) in Sections 4.1 and 4.2 is selected to compare with other forecasting methods. The compared methods include Neuro-Fuzzy model [37], ANFIS [38], RBF [39] and PM [40]. The Neuro-Fuzzy, ANFIS & RBF models are belonged to the

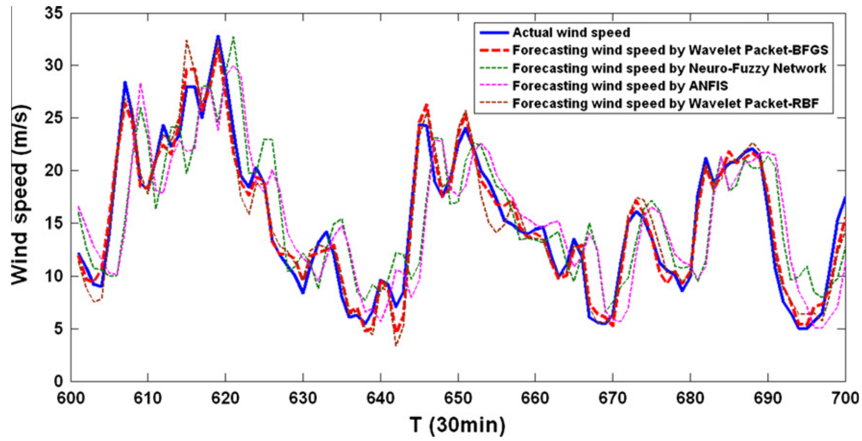

Fig. 26. Results of two-step prediction (5).

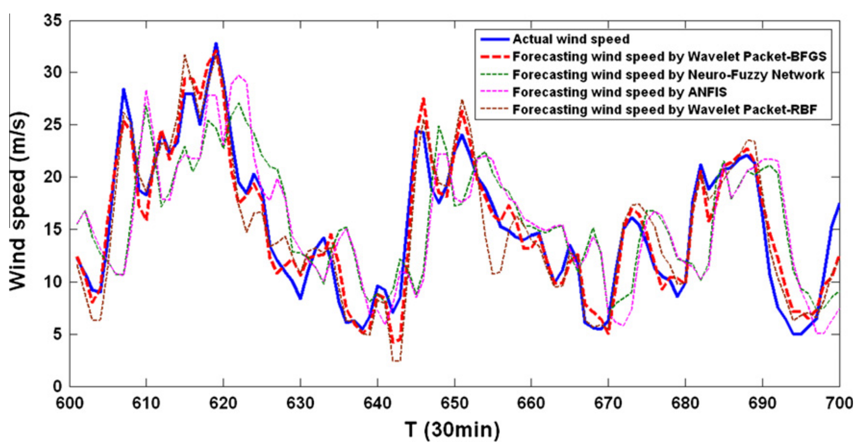

Fig. 27. Results of three-step prediction (5).

Table 7
Analysis of the forecasting results shown in Figs. 22–24.

Indexes	Wavelet Packet-BFGS			Wavelet-BFGS model			BFGS model		
	1-step	2-step	3-step	1-step	2-step	3-step	1-step	2-step	3-step
MAE (m/s)	0.4396	0.9624	1.3911	0.6608	1.2828	1.5415	1.9009	3.6957	4.9292
MAPE (%)	3.55	7.84	11.80	4.64	10.11	11.76	14.65	29.30	40.88
MSE (m/s)	0.5433	1.1594	1.7872	0.9004	1.6557	2.0396	2.4293	4.8393	6.1496

	Wavelet Packet-ARIMA-BFGS			ARIMA model		
	1-step	2-step	3-step	1-step	2-step	3-step
MAE (m/s)	0.4466	1.0054	1.5839	1.7684	3.6888	5.5465
MAPE (%)	3.53	8.04	12.41	13.43	27.31	45.10
MSE (m/s)	0.5777	1.2329	2.0968	2.3110	4.7987	6.8575

kind of artificial intelligence-based wind speed forecasting methods and the PM is a generally adopted statistical wind speed forecasting method.

The detailed computational steps of the Neuro-Fuzzy, ANFIS and RBF models can be found in Refs. [37–39], respectively. The computational steps of the PM are given as follows:

$$\widehat{X}_t(t) = X_t(t-1) + e_t, \quad t = 601, 602, \ldots, 700 \tag{5}$$

where $\{X_t\}$ is the original wind speed series and $\{e_t\}$ is a white noise series with zero mean and variance sigma.

In this study Matlab platform is selected to do the programming works for the computation of the different forecasting methods. In the forecasting programming, there are a series of Matlab toolbox functions adopted to facilitate the programming process, such as the 'ANFIS' function in the Fuzzy Logic toolbox for the ANFIS model and the 'NEWRB' function in the Neural Network toolbox for the RBF model. Figs. 17–19 show the results at 601st–700th data of one-step, two-step and three-step predictions. The estimated results of the predictions are given in Table 5. The MAPE and MSE errors in Table 6 are displayed in Fig. 20.

From Figs. 17–19 and Table 6, it can be seen that: (a) The bigger the number of forecast steps, the lower the accuracy; (b) the

Table 8
Analysis of the forecasting results shown in Figs. 25–27.

Indexes	Wavelet Packet-BFGS			Neuro-Fuzzy network			ANFIS		
	1-step	2-step	3-step	1-step	2-step	3-step	1-step	2-step	3-step
MAE (m/s)	0.4396	0.9624	1.3911	2.1462	3.6785	4.7997	2.3218	3.9593	4.9839
MAPE (%)	3.55	7.84	11.80	15.97	25.98	36.74	17.06	26.36	35.09
MSE (m/s)	0.5433	1.1594	1.7872	2.8226	4.7197	5.8802	3.0044	5.0569	6.1504
	Wavelet Packet-RBF			Persistent Model					
	1-step	2-step	3-step	1-step	2-step	3-step			
MAE (m/s)	0.5914	1.1370	1.7106	2.4296	–	–			
MAPE (%)	4.59	8.89	13.36	17.87	–	–			
MSE (m/s)	0.7476	1.4731	2.2378	3.1304	–	–			

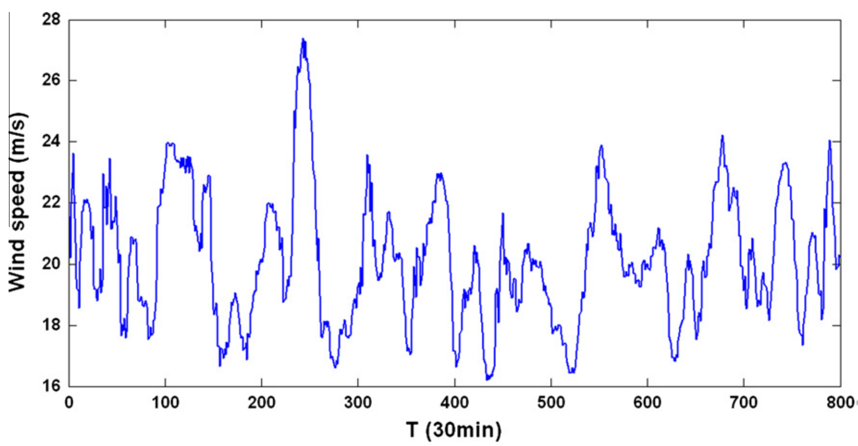

Fig. 28. Original wind speed series (3).

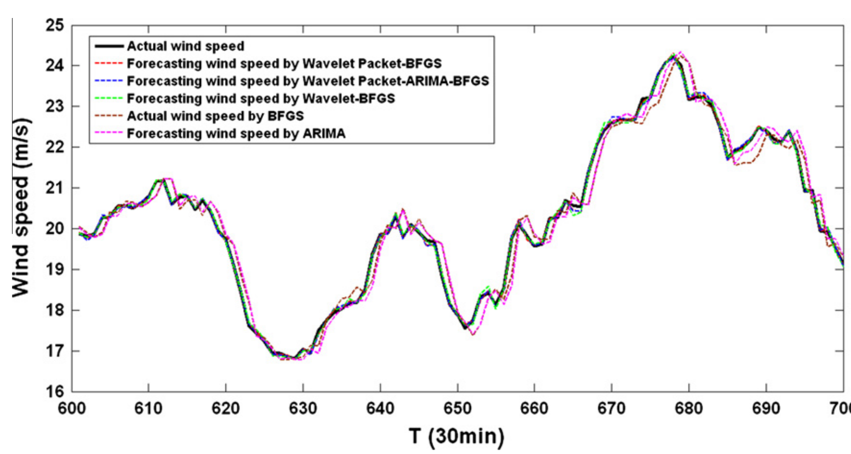

Fig. 29. Results of one-step prediction (6).

Wavelet Packet-BFGS is the best in this case. Due to the RBF is also a kind of neural networks, a Wavelet Packet-RBF is built to replace the pure RBF in this comparison. The results show that the performance of the Wavelet Packet-RBF is close to the Wavelet Packet-BFGS; and (c) the performance difference between the Neuro-Fuzzy and the ANFIS is not significant.

From Fig. 20, it can be found that the performance difference between the Wavelet Packet-BFGS and the Wavelet Packet-RBF becomes significant with the increase of the forecasting steps. It means the BFGS is more robust than the RBF in the multi-step predictions. At the same time compared to the Neuro-Fuzzy and ANFIS methods, the Wavelet Packet-BFGS has better performance in every forecasting step.

5. Additional forecasting cases

To further verify the performance presented in Section 4, another two sections of wind speed data named Case Two and Case Three from the same wind station at different seasons are used to establish models and make multi-step ahead predictions.

5.1. Case Two

The wind speed data in the Case Two are collected from February 10, 2012 to February 25, 2012, as displayed in Fig. 21. Obviously, this section of wind speed is strongly non-stationary. The

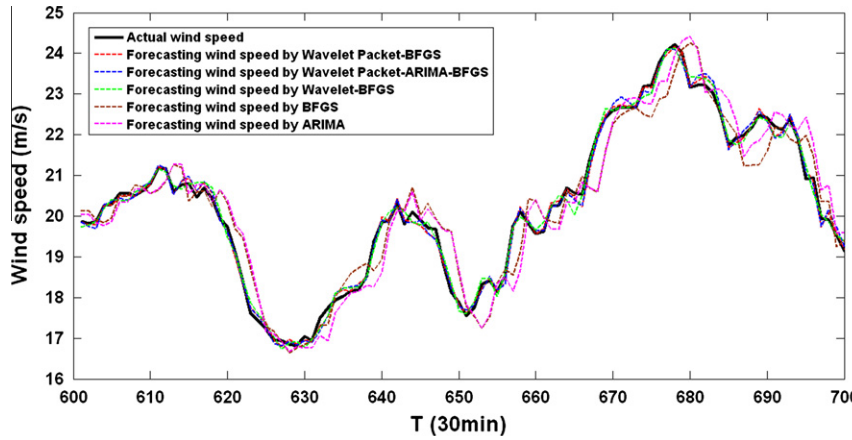

Fig. 30. Results of two-step prediction (6).

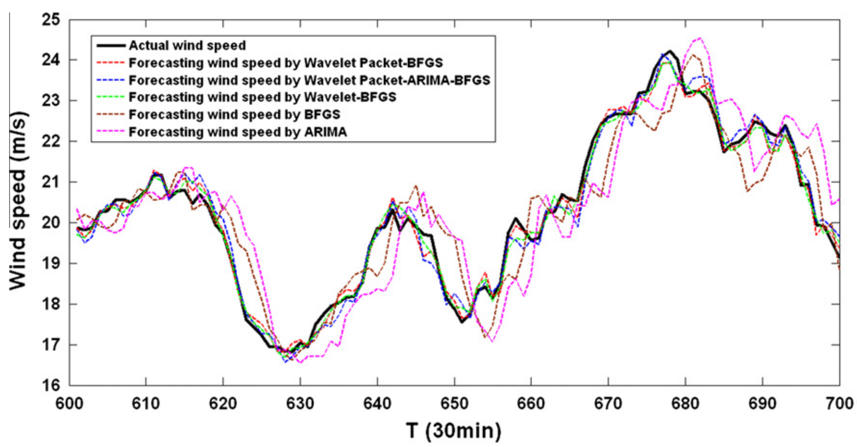

Fig. 31. Results of three-step prediction (6).

forecasting results are given in Figs. 22–27. Two groups of performance estimated results are given in Tables 7 and 8. Based on those results, the same conclusions to the Case One can be made.

5.2. Case Three

The wind speed data in the Case Three are collected from May 10, 2012 to May 25, 2012, as shown in Fig. 28. This section of wind speed is also strongly non-stationary. The forecasting results are demonstrated in Figs. 29–34. Two groups of performance estimated results are given in Tables 9 and 10. Based on those results, the same conclusions to the Case One and Case Two can be made.

6. Conclusions

Among the hybrid models presented in this study, the Wavelet Packet-BFGS model has the best performance. The primary reason of its good performance is that it employs the Wavelet Packet

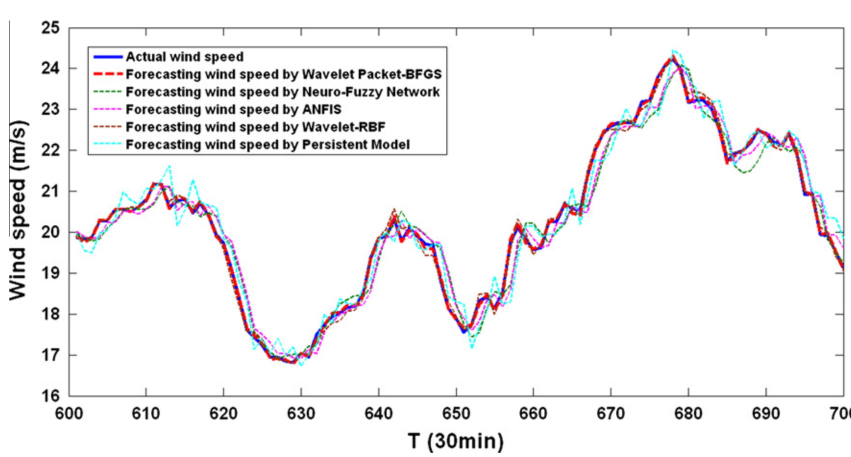

Fig. 32. Results of one-step prediction (7).

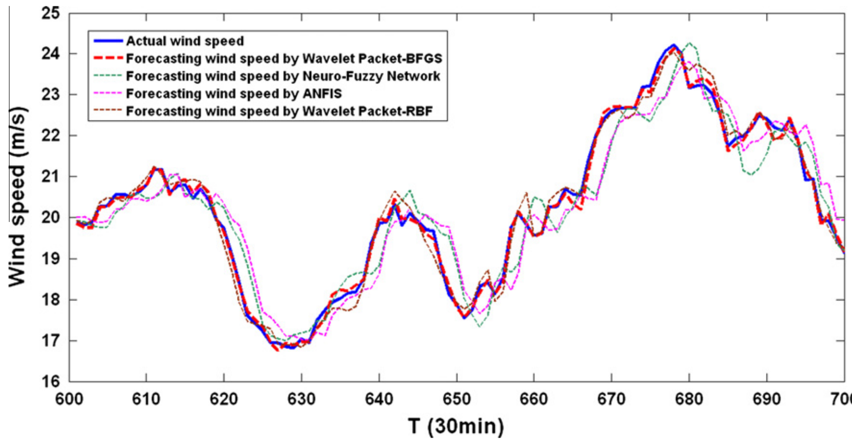

Fig. 33. Results of two-step prediction (7).

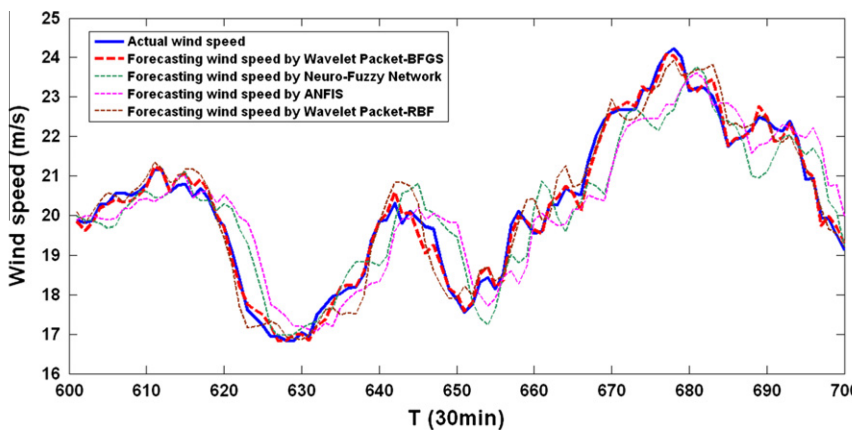

Fig. 34. Results of one-step prediction (7).

Table 9
Analysis of the forecasting results shown in Figs. 29–31.

Indexes	Wavelet Packet-BFGS			Wavelet-BFGS model			BFGS model		
	1-step	2-step	3-step	1-step	2-step	3-step	1-step	2-step	3-step
MAE (m/s)	0.0416	0.0961	0.1648	0.0620	0.1364	0.1789	0.2884	0.4553	0.5968
MAPE (%)	0.21	0.48	0.81	0.31	0.68	0.88	1.49	2.24	2.96
MSE (m/s)	0.0522	0.1176	0.2035	0.0767	0.1697	0.2236	0.3680	0.5820	0.7698
	Wavelet Packet-ARIMA-BFGS			ARIMA model					
	1-step	2-step	3-step	1-step	2-step	3-step			
MAE (m/s)	0.0458	0.1164	0.2194	0.2832	0.4783	0.8287			
MAPE (%)	0.28	0.57	1.09	1.41	2.37	4.16			
MSE (m/s)	0.0584	0.1388	0.2753	0.3766	0.6146	1.0167			

Table 10
Analysis of the forecasting results shown in Figs. 32–34.

Indexes	Wavelet Packet-BFGS			Neuro-Fuzzy network			ANFIS		
	1-step	2-step	3-step	1-step	2-step	3-step	1-step	2-step	3-step
MAE (m/s)	0.0416	0.0961	0.1648	0.3179	0.4897	0.6133	0.3109	0.5176	0.6840
MAPE (%)	0.21	0.48	0.81	1.57	2.41	3.02	1.55	2.58	3.43
MSE (m/s)	0.0522	0.1176	0.2035	0.4143	0.6226	0.7803	0.4050	0.6594	0.8680
	Wavelet Packet-RBF			Persistent Model					
	1-step	2-step	3-step	1-step	–	–			
MAE (m/s)	0.0988	0.1975	0.3227	0.3715	–	–			
MAPE (%)	0.49	0.98	1.06	1.85	–	–			
MSE (m/s)	0.1213	0.2485	0.3957	0.4592	–	–			

Decomposition to convert the non-stationary original wind speed into a series of sub-series data before the ANN component starts to predict. Although the Wavelet Packet-ARIMA-BFGS model has a little lower accuracy compared to the Wavelet Packet-BFGS model, its time performance is better because it uses the ARIMA models instead of the ANN models in approximation sub-series. Besides the Wavelet Packet-BFGS and Wavelet Packet-ARIMA-BFGS models, the hybrid Wavelet-BFGS model also has satisfactory performance.

Acknowledgements

The authors would like to thank the reviewers for their precious comments and suggestions which have been adopted to improve the quality of this paper. This study is supported by the Fundamental Research Funds for the Central Universities of China (Project No. 2012QNZT029) and the National Natural Science Foundation of China (Grant No. U1134203).

References

[1] Jinjin C. Development of offshore wind power in China. Renew Sustain Energy Rev 2011;15(9):5013–20.
[2] Kaneko T, Uehara A, Senjyu T, Yona A, Urasaki N. An integrated control method for a wind farm to reduce frequency deviations in a small power system. Appl Energy 2011;88(4):1049–58.
[3] Cassola F, Burlando M. Wind speed and wind energy forecast through Kalman filtering of numerical weather prediction model. Appl Energy 2012;99:154–66.
[4] Zhang WY, Wu J, Wang JZ, Zhao WG, Shen L. Performance analysis of four modified approaches for wind speed forecasting. Appl Energy 2012;99:324–33.
[5] Erdem E, Shi J. ARMA based approaches for forecasting the tuple of wind speed and direction. Appl Energy 2011;88:1405–14.
[6] Liu H, Tian HQ, Li YF. Comparison of two new ARIMA-ANN and ARIMA-Kalman hybrid methods for wind speed prediction. Appl Energy 2012;98:415–24.
[7] Liu HP, Erdem E, Shi J. Comprehensive evaluation of ARMA–GARCH(-M) approaches for modeling the mean and volatility of wind speed. Appl Energy 2011;88(3):724–32.
[8] Bouzgou H, Benoudjit N. Multiple architecture system for wind speed prediction. Appl Energy 2011;88(7):2463–71.
[9] Cao Q, Ewing BT, Thompson MA. Forecasting wind speed with recurrent neural networks. Eur J Oper Res 2012;221(1):148–54.
[10] Jiang Y, Song Z, Kusiak A. Very short-term wind speed forecasting with Bayesian structural break model. Renew Energy 2013;50:637–47.
[11] Guo ZH, Zhao WG, Lu HY, Wang JZ. Multi-step forecasting for wind speed using a modified EMD-based artificial neural network model. Renew Energy 2012;37(1):241–9.
[12] Salcedo-Sanz S, Ortiz-García EG, Pérez-Bellido ÁM, Portilla-Figueras A, Prieto L. Short term wind speed prediction based on evolutionary support vector regression algorithms. Expert Syst Appl 2011;38(4):4052–7.
[13] Guo ZH, Wu J, Lu HY, Wang JZ. A case study on a hybrid wind speed forecasting method using BP neural network. Knowl Based Syst 2011;24(7):1048–56.
[14] Liu HP, Shi J, Erdem E. Prediction of wind speed time series using modified Taylor Kriging method. Energy 2010;35(12):4870–9.
[15] Shi J, Guo JM, Zheng ST. Evaluation of hybrid forecasting approaches for wind speed and power generation time series. Renew Sustain Energy Rev 2012;16(5):3471–80.
[16] Haque AU, Mandal P, Kaye ME, Meng JL, Chang LC, Senjyu T. A new strategy for predicting short-term wind speed using soft computing models. Renew Sustain Energy Rev 2012;16(7):4563–73.
[17] Amjady N, Keynia F, Zareipour H. A new hybrid iterative method for short term wind speed forecasting. Eur Trans Electr Power 2011;21:581–95.
[18] Salim OM, Zohdy MA, Dorrah HT, Kamel AM. Adaptive neurofuzzy short-term wind-speed forecasting for Egypt's East-Coast. Int J Sustain Energy 2012. http://dx.doi.org/10.1080/14786451.2011.630468.
[19] Kani SAP, Ardehali MM. Very short-term wind speed prediction: a new artificial neural network–Markov chain model. Energy Convers Manage 2011;52(1):738–45.
[20] Zhou JY, Shi J, Li G. Fine tuning support vector machines for short-term wind speed forecasting. Energy Convers Manage 2011;52(4):1990–8.
[21] Hill DC, McMillan D, Bell KRW, Infield D. Application of auto-regressive models to UK wind speed data for power system impact studies. IEEE Trans Sustain Energy 2012;3(1):134–41.
[22] Amjady N, Keynia F, Zareipour H. Short-term wind power forecasting using Ridgelet neural network. Electr Power Syst Res 2011;81(12):2099–107.
[23] Amjady N, Keynia F, Zareipour H. Wind power prediction by a new forecast engine composed of modified hybrid neural network and enhanced particle swarm optimization. IEEE Trans Sustain Energy 2011;2(3):265–76.
[24] Maria Grazia De Giorgi, Ficarella A, Tarantino M. Assessment of the benefits of numerical weather predictions in wind power forecasting based on statistical methods. Energy 2011;36(7):3968–78.
[25] Colaka I, Sagiroglub S, Yesilbudakc M. Data mining and wind power prediction: a literature review. Renew Energy 2012;46:241–7.
[26] Shi J, Qu X, Zeng S. Short-term wind power generation forecasting: direct versus indirect ARIMA-based approaches. Int J Green Energy 2011;8(1):100–12.
[27] Bhaskar K, Singh SN. AWNN-assisted wind power forecasting using feed-forward neural network. IEEE Trans Sustain Energy 2012;3(2):306–15.
[28] Mohandes M, Rehman S, Rahman SM. Estimation of wind speed profile using adaptive neuro-fuzzy inference system (ANFIS). Appl Energy 2011;88(11):4024–32.
[29] Amjady N. Day-ahead price forecasting of electricity markets by a new fuzzy neural network. IEEE Trans Power Syst 2006;21(2):887–96.
[30] Mandal P, Senjyu T, Funabashi T. Neural networks approach to forecast several hour ahead electricity prices and loads in deregulated market. Energy Convers Manage 2006;47(15–16):2128–42.
[31] Mandal P, Srivastava AK, Park JW. An effort to optimize similar days parameters for ANN based electricity price forecasting. IEEE Trans Ind Appl 2009;45(5):1888–96.
[32] Mallat SG. A theory for multiresolution signal decomposition: the wavelet representation. IEEE Trans Pattern Anal Mach Intell 1989;11(7):674–93.
[33] Zhao XZ, Ye BY. Convolution wavelet packet transform and its applications to signal processing. Digital Signal Process 2010;20(5):1352–64.
[34] Vrahatis MN, Magoulas GD, Plagianakos VP. Convergence analysis of the Quickprop method. In: IEEE international joint conference on neural networks; 1999. p. 1209–14.
[35] Riedmiller M, Braun H. A direct adaptive method for faster backpropagation learning: the RPROP algorithm. In: IEEE international conference on neural networks; 1993. p. 586–91.
[36] Xia JH, Rusli, Kumta AS. Feedforward neural network trained by BFGS algorithm for modeling plasma etching of silicon carbide. IEEE Trans Plasma Sci 2010;38(2):142–8.
[37] Babuška R, Verbruggen H. Neuro-fuzzy methods for nonlinear system identification. Annu Rev Control 2003;27:73–85.
[38] Jang JSR. ANFIS: adaptive-network-based fuzzy inference systems. IEEE Trans Syst Man Cybernet 1993;23(3):665–85.
[39] Sfetsos A. A comparison of various forecasting techniques applied to mean hourly wind speed time series. Renew Energy 2000;21(1):23–35.
[40] Soman SS, Zareipour H, Malik O, Mandal P. A review of wind power and wind speed forecasting methods with different time horizons. In: IEEE north American power symposium; 2010. p. 1–8.